Bratislava Medical Journal (2025) 126:2116–2128
https://doi.org/10.1007/s44411-025-00233-2

RESEARCH

Comparative Cytotoxic Effects of Silver Nanoparticles Synthesized from *Humulus lupulus*, *Inula viscosa*, and *Olea europaea* on Saos-2 and MCF-7 Cells

Tuba Ozdemir-Sanci[1] · Busranur Ozalper[2] · Tuba Aydin[3] · Mustafa Gungormus[4]

Received: 2 April 2025 / Revised: 2 June 2025 / Accepted: 5 June 2025 / Published online: 13 June 2025

Abstract
Recent advances in green nanotechnology have enabled the development of plant-mediated silver nanoparticles (AgNPs) as promising anti-cancer agents. This study characterizes AgNPs biosynthesized using aqueous extracts of three medicinal plants—*Humulus lupulus* (hops), *Inula viscosa*, and *Olea europaea* (olive)—and evaluates their cytotoxic effects against Saos-2 osteosarcoma and MCF-7 breast cancer cell lines. Ultraviolet–Visible Spectroscopy (UV–Vis) confirmed nanoparticle formation through characteristic surface plasmon resonance (SPR) peaks (400–420 nm), while scanning electron microscopy revealed spherical particles (30–70 nm) with moderate aggregation. Additionally, X-ray diffraction (XRD) analysis confirmed the crystalline nature of the synthesized silver nanoparticles. The viability assay demonstrated significant dose- and time-dependent cytotoxicity, with *I. viscosa*-AgNPs showing particularly strong effects. Comparative analysis revealed plant-synthesized AgNPs exhibited enhanced biocompatibility and selective toxicity compared to chemically synthesized counterparts. The green synthesis approach employed in this study not only eliminates toxic chemical reductants but also enhances therapeutic potential through synergistic phytochemical-nanoparticle interactions. These results position plant-mediated AgNPs as a sustainable and effective alternative for targeting aggressive cancers like osteosarcoma and hormone-resistant breast cancer. The study highlights the importance of integrating traditional medicinal knowledge with modern nanotechnology for developing novel cancer therapeutics.

Keywords Cytotoxicity · *Humulus lupulus* · *Inula viscosa* · MCF-7 · *Olea europaea* · Saos-2 · Silver nanoparticles

1 Introduction

Cancer continues to be one of the most formidable health challenges of our time, accounting for nearly 10 million deaths globally in 2020 alone [1]. Among the diverse array of malignancies, osteosarcoma (OS) and breast cancer represent two particularly aggressive forms that pose significant therapeutic challenges. Osteosarcoma, the most common primary bone tumor, predominantly affects adolescents and young adults, with a propensity for early pulmonary metastasis and poor survival rates in advanced stages [2]. Despite multimodal treatment approaches combining surgery and chemotherapy, the 5-year survival rate for metastatic OS remains dismally low at 20–30% [3]. Similarly, breast cancer maintains its status as the most frequently diagnosed cancer in women worldwide, with hormone receptor-positive subtypes like MCF-7 accounting for approximately 70% of cases [4]. While significant advances have been made in targeted therapies, the emergence of treatment resistance and the debilitating side effects of conventional chemotherapeutics underscore the urgent need for novel therapeutic strategies [5]. In this context, nanotechnology has emerged as a revolutionary approach in cancer therapeutics, offering solutions to many limitations of traditional treatments [6]. Biosynthesized nanoparticles promise a therapeutic

✉ Tuba Ozdemir-Sanci
ozdemirsanci.tuba@aybu.edu.tr

1 Department of Histology and Embryology, Faculty of Medicine, Ankara Yıldırım Beyazıt University, Ankara, Türkiye

2 Department of Midwifery, Faculty of Health Sciences, Muş Alparslan University, Muş, Türkiye

3 Department of Pharmacognosy, Faculty of Pharmacy, Ağrı İbrahim Çeçen University, Ağrı, Türkiye

4 Department of Basic Sciences, Faculty of Dentistry, Ankara Yıldırım Beyazıt University, Ankara, Türkiye

revolution, offering targeted cancer drug delivery systems, potent antimicrobial effects, and reduced toxicity—paving the way for safer and more efficient treatments. As targeted drug carriers, nanoparticles improve therapeutic specificity and minimize side effects, with biosynthesized variants offering additional biocompatibility and multifunctionality for advanced therapies. [7, 8].

Silver nanoparticles are a major research focus due to their unique physicochemical properties—such as high surface area and tunable optical behavior—along with their ability to selectively target cancer cells [9]. AgNPs exert their anticancer activity via diverse processes, such as ROS (radical oxygen species) accumulation, impaired energy metabolism, and activation of apoptotic pathways. The clinical potential of AgNPs is further highlighted by their ability to circumvent multidrug resistance mechanisms, which commonly compromise the effectiveness of conventional anticancer drugs [10]. Traditional methods for AgNPs synthesis often rely on physical (e.g., laser ablation, evaporation–condensation) or chemical methods (e.g., chemical reduction using sodium borohydride or hydrazine) which raise concerns regarding toxicity, environmental impact, and potential harm to healthy tissues. In recent years, green synthesis has emerged as a sustainable and eco-friendly alternative for the production of AgNPs [11]. Unlike conventional methods, green synthesis utilizes biological entities such as plant extracts, fungi, bacteria, and biomolecules to reduce metal ions into stable nanoparticles. Among biological routes, plant-mediated synthesis is particularly attractive due to the presence of diverse phytochemicals—such as polyphenols, flavonoids, terpenoids, alkaloids, and proteins—that function both as reducing agents and stabilizers [12, 13]. These naturally occurring compounds eliminate the need for additional capping or toxic reducing agents and facilitate the formation of nanoparticles under mild conditions. Moreover, green-synthesized nanoparticles often exhibit improved biocompatibility, colloidal stability, and functional versatility of the phytochemicals [13–15].

This study focuses on three medicinal plants with well-documented anticancer properties: *Humulus lupulus (hops), Inula viscosa*, and *Olea europaea* (olive). *H. lupulus*, best known for its use in brewing, contains high concentrations of xanthohumol, a prenylated flavonoid that has demonstrated remarkable antiproliferative effects against various cancer types through multiple mechanisms including cell cycle arrest and apoptosis induction [16]. The Mediterranean herb *I. viscosa*, traditionally used in folk medicine, is abundant in sesquiterpene lactones like tomentosin, exhibiting cancer-specific cytotoxicity with minimal effects on normal cells [17]. *O. europaea* leaves contain oleuropein, a phenolic compound with demonstrated anticancer activity through its antioxidant, anti-inflammatory, and pro-apoptotic properties [18]. The selection of these plants was based not only on their phytochemical richness but also on their potential to enhance the anticancer properties of AgNPs through synergistic interactions.

This study aims to synthesize and characterize AgNPs using aqueous extracts of *H. lupulus*, *I. viscosa*, and *O. europaea*, and to evaluate their cytotoxic and potential pro-apoptotic effects against Saos-2 osteosarcoma and MCF-7 breast cancer cell lines. While many studies have focused on the green synthesis of AgNPs using individual plant species, comparative studies that control for synthesis parameters are scarce. By applying a standardized synthesis and characterization protocol, we aimed to systematically assess how phytochemical composition influences nanoparticle properties and biological activities, which represents a knowledge gap in the field. This comparative approach provides deeper insights into the selection and optimization of plant sources for tailored nanoparticle synthesis. The investigation focuses on elucidating dose- and time-dependent responses, with particular attention to phytochemical-nanoparticle interactions that may inhibit cell proliferation, and trigger apoptosis in cancer cells.

2 Materials and Methods

2.1 Botanical Material Acquisition and Authentication

The plant materials used in this study included *Humulus lupulus* (hop cones*), Inula viscosa* (leaves), and *Olea europaea* (olive leaves). The hop cones were obtained from the Bilecik Pazaryeri District Directorate of Agriculture in Türkiye. The aerial parts of *Inula viscosa* and leaves of *Olea europaea* were collected from the Hatay Provincial Center in Türkiye.

2.2 Preparation of Plant Extracts

The water extracts of the plant materials were prepared using a standardized protocol. Briefly, 100 g of each plant material (hop cones, *Inula viscosa* leaves, and *Olea europaea* leaves) were weighed and combined with 500 ml of distilled water heated to 60 °C. The mixture was stirred continuously for one hour using a magnetic stirrer on a temperature-controlled hot plate to ensure proper extraction of phytochemicals. Following the stirring process, the mixture was cooled to ambient temperature (25 °C) and subsequently subjected to filtration through Whatman filter paper No. 41 (Merck & Co., Kenilworth, NJ, USA) for removal of particulate contaminants. The filtered solution was gathered and refrigerated at 4 °C for subsequent applications. To maintain reproducibility and bioactivity, new extract preparations were made for every nanoparticle synthesis batch.

2.3 Synthesis of Silver Nanoparticles

2.3.1 Chemical Synthesis of AgNPs (Control Group)

Chemically synthesized silver nanoparticles (AgNPs) were prepared as a reference control group using the classical sodium borohydride ($NaBH_4$) reduction method, in accordance with established protocols [19]. Briefly, a cold aqueous solution containing 20 mM trisodium citrate (Sigma-Aldrich, ≥ 99% purity) and 2 mM freshly prepared $NaBH_4$ (Sigma–Aldrich, ≥ 98% purity) was prepared in double-distilled water and maintained in an ice bath (4 °C) to minimize the decomposition of the reducing agent. Subsequently, 1 mM aqueous $AgNO_3$ (silver nitrate, Merck, ≥ 99.9% purity) was added dropwise (~ 1 drop/sec) under vigorous magnetic stirring at 1000 rpm. Upon addition of Ag^+, an immediate yellowish-brown color developed, indicating the formation of silver nanoparticles through the reduction of Ag^+ to Ag^0 by $NaBH_4$, facilitated by citrate ions acting as stabilizing/capping agents. The reaction was allowed to proceed for 30 min to ensure complete reduction. The resulting pellet was washed twice with ultrapure distilled water to remove excess reactants and unbound ions. The purified nanoparticles were subsequently dried under vacuum at 40 °C for 24 h using a vacuum oven, yielding a fine dark grey powder of chemically synthesized AgNPs.

2.3.2 Plant-Based (Green) Synthesis of AgNPs

The silver nanoparticles were synthesized using an eco-friendly approach leveraging the dual reducing and stabilizing capabilities of aqueous extracts from *Humulus lupulus* (hops), *Inula viscosa, and Olea europaea*. These medicinal plants were selected for their high phenolic content (flavonoids, terpenoids, and tannins), which facilitate electron transfer for Ag^+ ion reduction while naturally capping the nanoparticles to prevent aggregation. For the synthesis, plant materials were shade-dried, powdered, and extracted with distilled water (1:10 w/v) at 60 °C for 2 h, with the filtrate lyophilized to concentrate bioactive compounds. In the optimized protocol, 10 ml of each extract was reacted with 1 mM $AgNO_3$ solution (added dropwise at 1 ml/min) at 60 °C under constant stirring (800 rpm). The reaction progress was monitored via UV–Vis spectroscopy, with the characteristic surface plasmon resonance peak at ~ 420 nm and color change from pale yellow to deep brown confirming AgNP formation after 30 min. The mixture was then centrifuged at 5000 rpm for 1 h at 4 °C, followed by three washing steps using a 1:1 mixture of distilled water and ethanol to remove organic residues. Finally, the samples were vacuum-dried at 40 °C for 24 h to obtain stable silver nanoparticle powders.

2.4 Nanostructural Characterization of AgNPs

2.4.1 Spectrophotometric Profiling of AgNPs

UV–Vis spectroscopy confirmed AgNP formation and stability spectral analysis (300–600 nm) was performed on the nanoparticles using a spectrophotometer (Fischer Scientific Inc., Hampton, NY, USA) to determine their optical absorption characteristics. The characteristic surface plasmon resonance peaks for AgNPs were observed at around 400–420 nm, indicating the successful synthesis of nanoparticles [19].

2.4.2 High-Resolution Morphological Profiling Using SEM

The morphological characteristics and surface topography of the biosynthesized silver nanoparticles were analyzed using Scanning Electron Microscopy (SEM). A small amount of dried AgNP sample was mounted onto a carbon-coated copper grid and sputter-coated with a thin layer of gold to enhance conductivity. The samples were then examined under a high-resolution SEM (Hitachi, SU5000). SEM images were used to evaluate particle size, shape, and distribution to confirm the successful formation of nanoscale silver structures.

2.4.3 X-Ray Diffractometry

X-ray diffraction measurements were carried out using a Rigaku Miniflex 600 diffractometer (Rigaku Corporation, Tokyo, Japan), operating with Cu Kα radiation ($\lambda = 0.154056$ nm), at an accelerating voltage of 40 kV and a current of 15 mA. The diffraction patterns were recorded over a 2θ range of 20–80°, with a step size of 0.01° and a scanning rate of 1° per minute.

2.5 Cell Culture

The Saos-2 osteosarcoma and MCF-7 breast adenocarcinoma cell lines were procured from ATCC (Manassas, VA, USA). Cells were grown in DMEM (Gibco, Thermo Fisher Scientific) enriched with 10% heat-inactivated FBS (Biochrom AG) and 1% penicillin–streptomycin antibiotic cocktail (Sigma-Aldrich). Cultures were kept at 37 °C in a 5% CO_2 humidified atmosphere (Thermo Scientific), with medium refreshed every 48–72 h. Subculturing was performed at 80–90% confluence using 0.25% trypsin–EDTA (Gibco, Thermo Fisher Scientific).

2.6 Cytotoxicity Assay (XTT Assay)

AgNP cytotoxicity was determined by XTT (2,3-Bis-(2-methoxy-4-nitro-5-sulfophenyl)−2H-tetrazolium-5-carboxanilide) viability assay (Biotium, USA) [20] using Saos-2 and MCF-7 cells. Cells (3×10^4/well) were cultured in 96-well plates for 24 h to ensure proper attachment before nanoparticle exposure. They were then treated with AgNPs synthesized from *H. lupulus, I. viscosa*, and *O. europaea* at 1:1, 1:5, and 1:10 dilutions for 24 and 48 h. After treatment, 50 µl of XTT solution was added to each well, followed by 4 h incubation at 37 °C. Absorbance readings at 460 nm were acquired with a Varioskan Flash microplate spectrophotometer. (Fischer Scientific Inc., USA). Viability results are presented as percentages relative to control cells. All experiments were conducted in triplicate.

2.7 Statistical Analysis

The cytotoxic effects were quantitatively evaluated using GraphPad Prism (Version 8.4.2). Data from three independent biological replicates (each performed in technical triplicate) are expressed as mean ± standard deviation (SD). Dose- and time-dependent responses were evaluated via two-way ANOVA, with treatment concentration and exposure duration as independent variables, followed by Tukey's post hoc test for pairwise comparisons. In all analyses, a probability threshold of $p < 0.05$ served as the criterion for establishing statistical significance.

3 Results and Discussion

3.1 Synthesis of Silver Nanoparticles

In this study, water extracts of *Humulus lupulus* (cones), *Inula viscosa* (leaves), and *Olea europaea* (leaves) were used for the biosynthesis of silver nanoparticles. Phytochemical-mediated reduction of silver ions was visually demonstrated through a rapid color shift to brown, characteristic of surface plasmon resonance in formed AgNPs. This color change is attributed to the reduction of Ag^+ ions to Ag^0 by the phytochemicals present in the plant extracts, which act as both reducing and stabilizing agents [21, 22] (Fig. 1).

3.2 Spectrophotometric Profiling of AgNPs

The formation of AgNPs was further confirmed by UV–Vis spectroscopy, which is a widely used technique for characterizing metallic nanoparticles due to their unique surface plasmon resonance (SPR) properties. UV–Vis spectroscopy was performed using a Varioskan Flash micro-plate reader in the wavelength range of 300–700 nm, with a scanning interval of 1 nm and baseline correction applied using deionized water as a blank. The UV–Vis spectra of the reaction solutions containing AgNPs synthesized using $NaBH_4$, *H. lupulus, I. viscosa,* and *O. europaea* extracts exhibited characteristic absorbance peaks at 388 nm, 400 nm, 420 nm, and 400 nm, respectively (Fig. 2). These peaks are consistent with the SPR band of AgNPs, confirming their successful synthesis [22]. The slight variations in the λmax values can be attributed to differences in the shape, size and stabilizing agents of the nanoparticles synthesized using different plant extracts.

3.3 X-Ray Diffractometry

The XRD patterns displayed distinct diffraction peaks at 38.36°, 44.63°, 55.20°, 57.75°, 64.73° and 77.59° corresponding to the (111), (200), (220), and (311) planes of face-centered cubic (fcc) silver, respectively, in accordance with the JCPDS file 04–0783, indicating the crystalline nature of the nanoparticles. Additional peaks related to AgO, and Ag_2O phases were also observed. Peaks related to AgO observed at 32.47 and 46.52°, corresponding to the (111) and (211) planes matched the JCPDS file 84–1108, while those attributed to Ag_2O at 28, 32.47, 38.36, 46.48, 55.16, 55.81, 57.81, 67.77° and 74.98° corresponding to the (110), (111), (200), (211), (220), (221), (013), and (311) planes, respectively, were consistent with JCPDS file 76–1393. Moreover, the XRD peak positions and assigned phases are consistent with previous studies that reported similar crystalline patterns for green-synthesized silver nanoparticles using plant extracts, further supporting the validity of our findings [23–25]. When $NaBH_4$ was used as the reducing agent, AgNP peaks were more prominent relative to the other phases. In contrast, AgO peaks were more prominent relative to the other phases in the I-AgNPs. Ag_2O peaks were the least prominent in all groups (Fig. 3).

3.4 High-Resolution Morphological Profiling

Morphological characterization of the biosynthesized AgNPs was conducted using high-resolution scanning electron microscopy. Scanning electron microscopy images revealed that the AgNPs synthesized from all three plant extracts were mostly spherical in shape and exhibited nanoscale morphology. The particles showed moderate aggregation but maintained distinguishable individual boundaries. Particle sizes were estimated to be within the range of 30–70 nm for each formulation. The particle sizes were estimated based on SEM micrographs and the SPR absorption maxima observed in UV–Vis spectra. SEM images provided a direct visualization of nanoparticle morphology, allowing for the approximation of average particle size The SPR peaks, which typically shift to longer

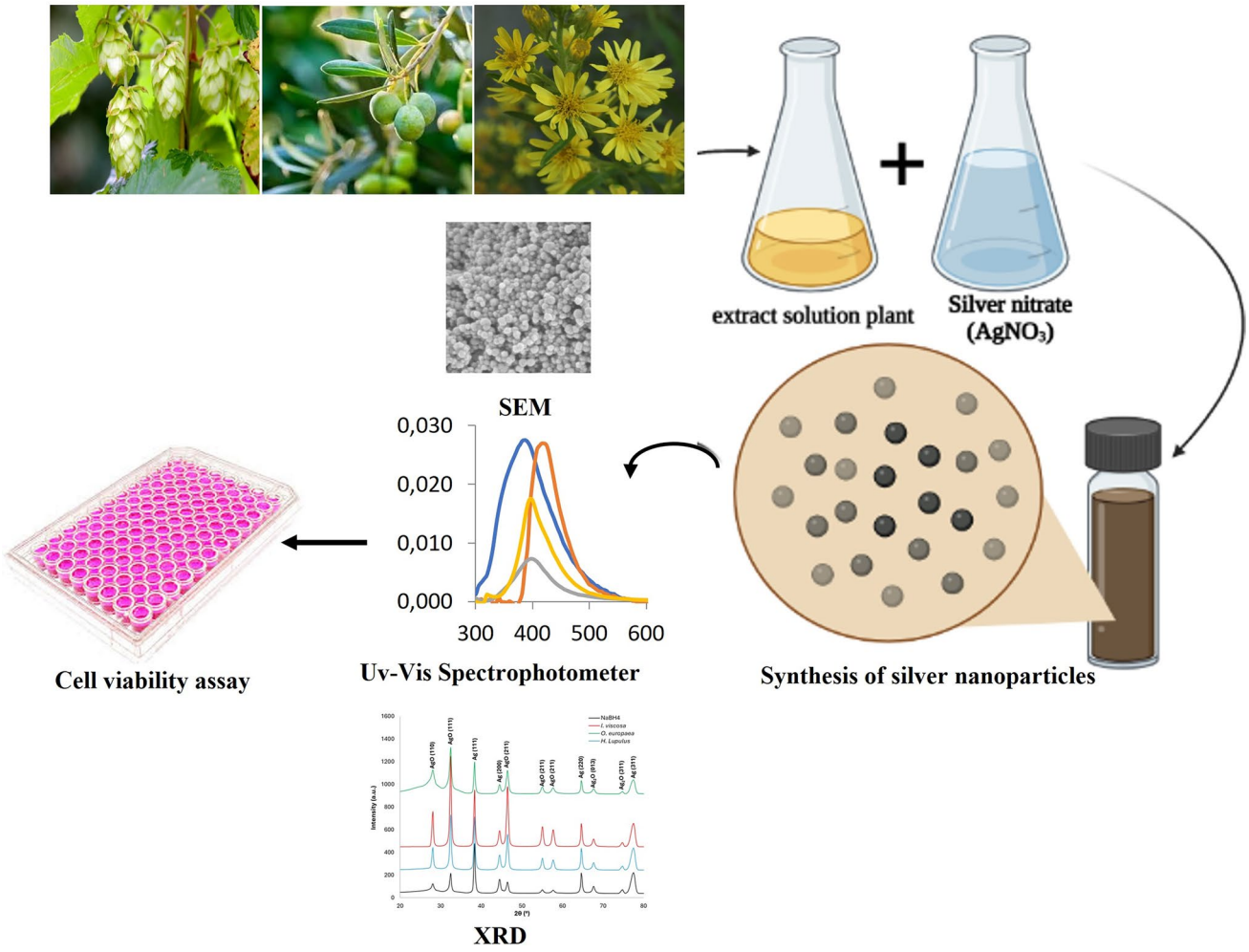

Fig. 1 Overview of the plant-based synthesis and characterization process of AgNPs. Representative diagram showing the biosynthesis of AgNPs using water extracts of *Humulus lupulus, Olea europaea*, and *Inula viscosa*

wavelengths as particle size increases, were used as an indirect size indicator. Based on the λ_max values and established correlations in the literature, the particle sizes were estimated to be in the range of 30–70 nm.

3.5 Dose-Dependent Cytotoxic Effect of AgNPs in Saos-2 and MCF-7 Cells

The cytotoxic effects of three biologically synthesized AgNPs (I-AgNPs, H-AgNPs, and O-AgNPs) were systematically evaluated in Saos-2 and MCF-7 cell lines through XTT viability assays. The optical density measurements at 460 nm (OD_{460}) revealed significant differences in cellular responses depending on nanoparticle formulation, concentration, and exposure duration (Figs. 4 and 5).

The time-dependent enhancement of cytotoxicity is clearly illustrated in Figs. 4 and 5, which present the OD_{460} measurements for Saos-2 and MCF-7 cells, respectively. The cytotoxic potential of the different nanoparticle formulations was quantitatively compared through IC_{50} determinations. I-AgNPs demonstrated the lowest IC_{50} values in both cell lines, measuring 0.38 mg/ml in Saos-2 cells and 0.52 mg/ml in MCF-7 cells after 24 h of exposure. These values decreased to 0.25 mg/ml and 0.37 mg/ml respectively following 48 h of treatment. H-AgNPs showed intermediate potency, with IC_{50} values of 0.52 mg/ml (Saos-2) and 0.67 mg/ml (MCF-7) at 24 h, declining to 0.34 mg/ml and 0.49 mg/ml after 48 h. O-AgNPs consistently required the highest concentrations to achieve equivalent cytotoxic effects, exhibiting IC_{50} values of 0.68 mg/ml in Saos-2 cells and 0.82 mg/ml in MCF-7 cells at 24 h, which reduced to 0.45 mg/ml and 0.61 mg/ml respectively at the 48 h time point.

I-AgNPs maintained greater potency than H-AgNPs and O-AgNPs across both cell lines and time points ($p < 0.05$ for

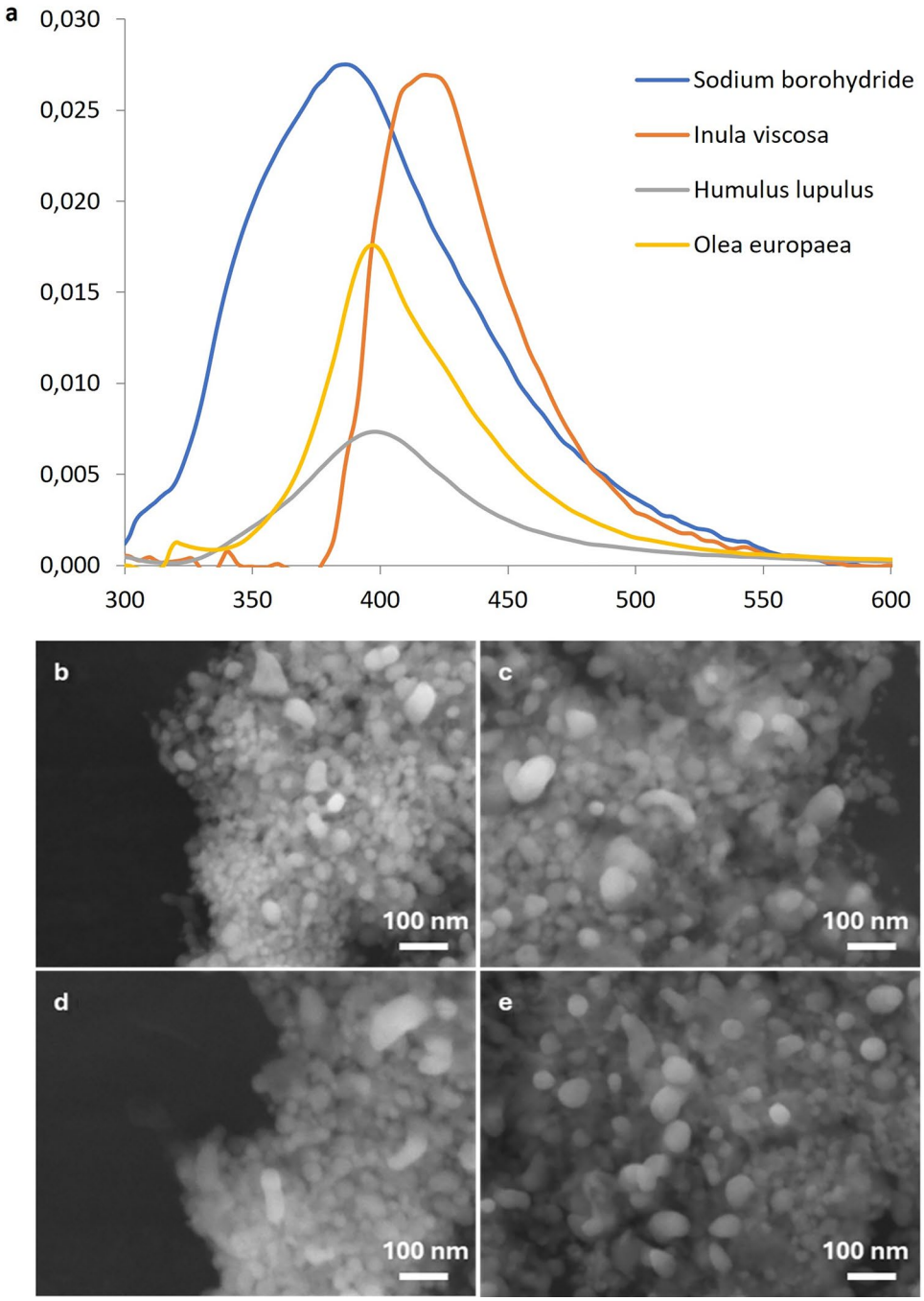

Fig. 2 Characterization of biosynthesized AgNPs using ultraviolet–visible spectrophotometer and high-resolution scanning electron microscopy. **a** UV–Vis absorption spectra of AgNPs synthesized from *Humulus lupulus, Inula viscosa*, and *Olea europaea* water extracts. b-e) SEM images of biosynthesized AgNPs using $NaBH_4$ (**b**), *H. lupulus* (**c**), *I. viscosa* (**d**), and *O. europaea* (**e**), respectively

all comparisons). Saos-2 cells consistently showed greater sensitivity than MCF-7 cells, requiring lower nanoparticle concentrations to achieve equivalent cytotoxic effects.

The MCF-7 cell line demonstrated greater resistance to nanoparticle-induced cytotoxicity, as evidenced by systematically higher OD_{460} values across all experimental conditions. At the 1:1 dilution, I-AgNPs reduced MCF-7 viability after 24 and 48 h, representing significantly less cytotoxicity than observed in Saos-2 cells ($p < 0.01$ for both time points). This pattern of differential sensitivity was maintained for H-AgNPs and O-AgNPs, with MCF-7 cells consistently showing higher viability than Saos-2 cells when treated with equivalent nanoparticle concentrations.

According to the data obtained, as a result of dose- and time-dependent comparisons of live cell rates, the cytotoxic potential of biogenic silver nanoparticles follows a consistent hierarchy (I-AgNPs > H-AgNPs > O-AgNPs) in both cell lines. Saos-2 cells are significantly more sensitive to nanoparticle-induced cytotoxicity than MCF-7 cells (Fig. 6). All formulations show enhanced cytotoxicity with prolonged

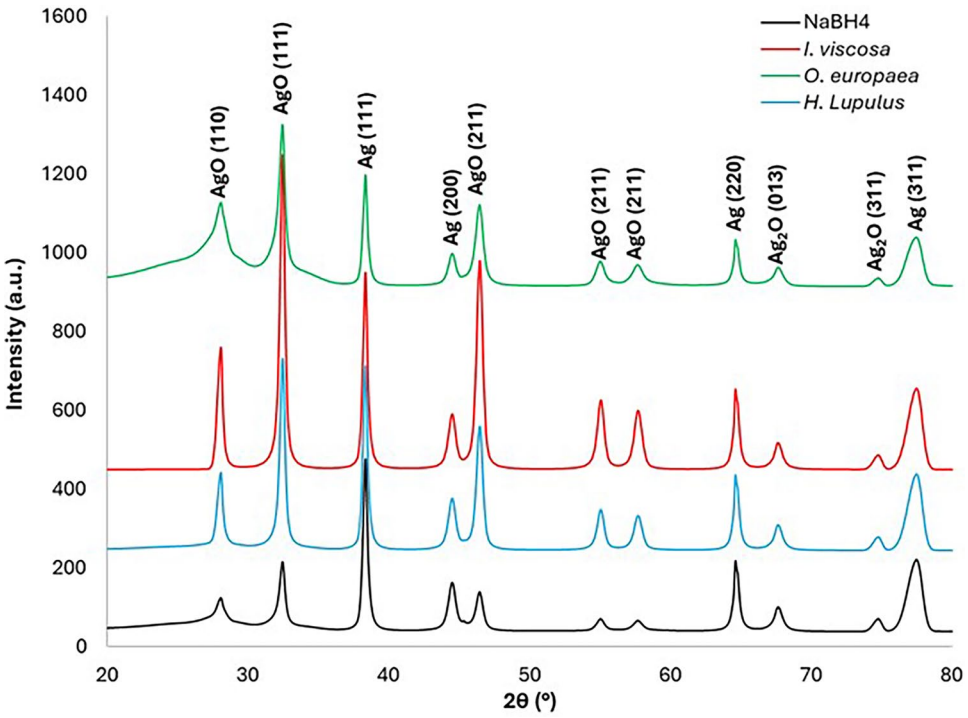

Fig. 3 X-Ray Diffractograms of the synthesized particles

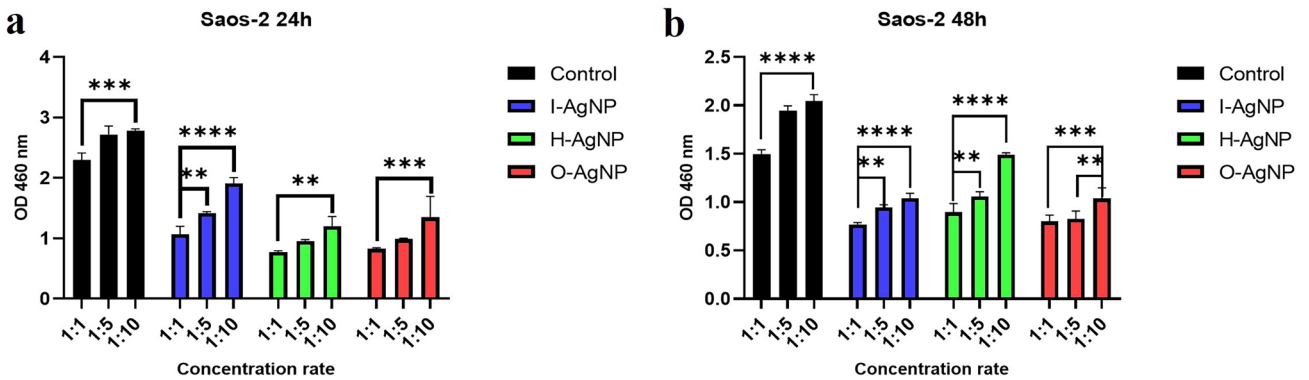

Fig. 4 Dose- and time-dependent cytotoxicity of biosynthesized AgNPs in Saos-2 cells. Cells were treated with 1:1, 1:5, and 1:10 dilutions for 24 and 48 h. $NaBH_4$-synthesized AgNPs were included. Data represent mean ± SD (n = 3); **p < 0.01, ***p < 0.001 ****p < 0.0001 vs. negative control

exposure, and the differential effects between nanoparticle formulations are maintained across concentrations and exposure durations.

4 Discussion

Cancer burden estimates for 2020 indicated about 19.3 million newly developed cases and 10 million fatalities attributable to malignant neoplasms. Rising global cancer incidence underscores the demand for novel therapies [26]. Bioactive compounds obtained from plants play important roles in the chemoprevention of cancer. Phytochemicals are promising agents for increasing treatment effectiveness and reducing side effects in cancer patients. Various phytochemicals have undergone clinical trials to determine their cancer chemopreventive effects [27]. However, phytochemicals may have disadvantages such as low solubility, poor penetration into cells, high hepatic distribution, and a narrow therapeutic index. To overcome these limitations, the conjugation of phytochemicals with natural product-based nanoformulations has been recommended. The combination of phytochemicals with nano-structures is a crucial step toward increasing their bioavailability [28–30].

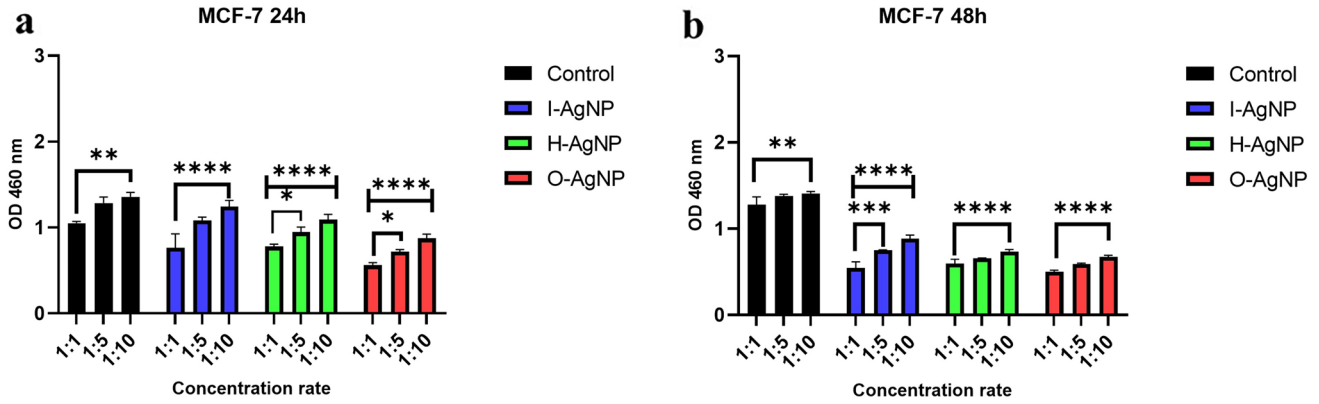

Fig. 5 Dose- and time-dependent cytotoxicity of biosynthesized AgNPs in MCF-7 cells. Cells were treated with 1:1, 1:5, and 1:10 dilutions for 24 and 48 h. $NaBH_4$-synthesized AgNPs (negative control) were included. Data represent mean ± SD (n = 3); *p < 0.05, **p < 0.01, ***p < 0.001 ****p < 0.0001 vs. negative control

In this study, silver nanoparticles were successfully synthesized using water extracts of *H. lupulus*, *I. viscosa*, and *O. europaea* through a green synthesis approach. The spectrophotometric analysis and high-resolution scanning electron microscopy analysis confirmed nanoparticle formation, and cytotoxicity assays demonstrated that the biosynthesized AgNPs exhibited significant, dose- and time-dependent antiproliferative effects against Saos-2 and MCF-7 cell lines. Although SEM imaging showed predominantly spherical particles in shape, slight variations were observed in the surface plasmon resonance peaks measured by UV–Vis spectroscopy, with λmax values ranging from 388 to 420 nm. The SPR peak position is influenced not only by nanoparticle shape but also by particle size, size distribution, aggregation state, and surface chemistry. In particular, even small differences in mean diameter can shift the λmax due to altered conduction electron oscillation at the nanoparticle surface. Furthermore, each plant extract contains a distinct profile of phytochemicals that act as reducing and capping agents during synthesis. These bioactive compounds form a surface corona around the nanoparticles and create unique dielectric environments, which influence the optical absorption properties. Therefore, the observed λmax shifts are consistent with the formation of spherical but chemically distinct AgNPs, each shaped by the molecular composition of the corresponding plant extract.

XRD analysis showed that the synthesized particles contained multiple phases. Among these, AgO and Ag_2O are known as the two stable forms of silver oxide, both of which can undergo reduction to yield elemental silver [31]. Similar to metallic AgNPs, silver oxides exhibit notable cytotoxic activity [32, 33], and in some reports, their activity surpasses that of pure silver nanoparticles [34]. Consequently, the presence of oxide forms rather than exclusively metallic silver was not considered a limitation in this study. The higher prominence of silver oxide phases in the AgNPs synthesized using plant extracts can be attributed to the nature and strength of the reducing agents involved. The green synthesis of AgNPs is facilitated by phytochemicals present in the aqueous plant extracts, which serve as both reducing and capping agents. Flavonoids (e.g., xanthohumol in *Humulus lupulus*), phenolic compounds (e.g., oleuropein and hydroxytyrosol in *Olea europaea*), and sesquiterpene lactones (e.g., tomentosin in *Inula viscosa*) are well-documented to possess redox-active functional groups, such as hydroxyl and carbonyl, which can donate electrons to reduce Ag^+ to Ag^0. This redox reaction is typically accompanied by the oxidation of these compounds to quinone-like structures. Simultaneously, these phytochemicals adsorb onto the surface of newly formed nanoparticles, preventing aggregation and enhancing stability [35, 36]. However, as the XRD findings suggest, these compounds may not fully reduce Ag^+ ions to elemental silver, leading to the formation of partially reduced products like Ag_2O and AgO. In contrast, $NaBH_4$ is a stronger reducing agent that promotes a more complete reduction of silver ions to metallic Ag, thereby favoring the formation of AgNPs over oxide forms. These factors may explain the greater abundance of silver oxide phases in biosynthesized nanoparticles.

Among the tested plant-mediated nanoparticles, I-AgNPs showed the most pronounced cytotoxicity. AgNPs are known to induce cellular stress by generating excessive ROS, which can damage proteins, lipids, and DNA. This oxidative stress disrupts mitochondrial membrane potential, leading to cytochrome c release and activation of intrinsic apoptotic pathways [36, 37]. The proposed synergistic interaction between the known mechanisms of silver nanoparticle-induced cytotoxicity and the intrinsic bioactivity of the tested phytochemicals are discussed below.

In our study, H-AgNPs exhibited cytotoxic effects against Saos-2 and MCF-7 cell lines, particularly at the 24 h time point. In our study, the effects of silver nanoparticles

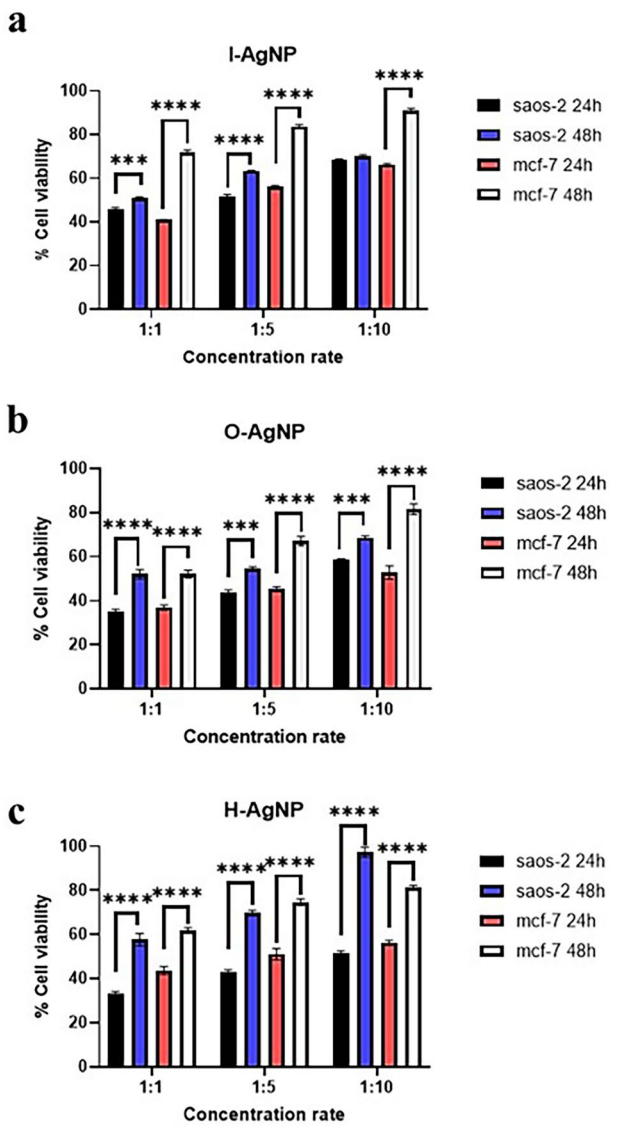

Fig. 6 Comparative percentage of cell viability of three plant-based AgNPs formulations (I-AgNPs, H-AgNPs, O-AgNPs) in Saos-2 and MCF-7 cell lines after 24 and 48 h exposures. Data represent mean ± SD of three independent experiments (n = 3). **p < 0.01, ***p < 0.001, ****p < 0.0001

containing on Saos-2 osteosarcoma and MCF-7 cell viability were examined. It was observed that H-AgNPs showed cytotoxic effects against Saos-2 and MCF-7 cell lines, especially at the 24th hour. *H.lupulus* produces important phytochemicals with various biological activities. Monteiro et al. reported that flavonoids obtained from *Humulus lupulus* reduced cell viability in Sk-Br-3 breast cancer cells by modulating aromatase activity, a key enzyme in estrogen biosynthesis, which plays a role in hormone-dependent breast cancer progression [38]. Similarly, Önder et al. investigated the effects of different *Humulus lupulus* extracts on Hep3B hepatocellular carcinoma and HT-29 colon cancer cells. Their findings indicated that methanol-1 extract significantly inhibited Hep3B cell proliferation by 70% at doses of 0.6–1 mg/ml, suggesting a strong antiproliferative activity [39]. Furthermore, Caban et al. demonstrated that *Humulus lupulus* extract inhibited angiogenesis, invasion, and migration with a significant reduction in SW-480 and HT-29 cell invasion and migration following incubation with the extract [40]. In addition, Ho et al. showed that xanthohumol, a flavonoid derived from *Humulus lupulus*, reduced proliferation in hepatocellular carcinoma cell lines to activate caspase-9 and caspase-3, triggering mitochondrial apoptosis [41]. Das et al. synthesized silver nanoparticles containing *Humulus lupulus* ethanol extract and reported its anticancer effect on MCF-7 cells, while also demonstrating minimal cytotoxicity towards normal cells. These effects can be attributed to a synergistic interaction between the intrinsic bioactivity of *H. lupulus* phytochemicals and the known mechanisms of silver nanoparticle-induced cytotoxicity. This pathway is particularly relevant in MCF-7 cells, which are partially deficient in caspase-3, yet respond to mitochondrial stress through alternative apoptotic signals [42, 43]. Xanthohumol can also arrest the cell cycle at the G0/G1 or G2/M phases by modulating cyclin-dependent kinase activity and suppressing growth factor signaling [44]. Collectively, these mechanisms support the potent cytotoxic effects observed in this study, particularly at 24–48 h of nanoparticle exposure. Future studies involving transcriptomic or proteomic analyses may further elucidate the molecular signatures associated with H-AgNP treatment in osteosarcoma and breast cancer models.

The examination of I-AgNP showed a significantly reduced cell viability in the investigated cell lines. The time-dependent enhancement of cytotoxicity was most pronounced for I-AgNPs, suggesting its particularly rapid cellular internalization or activation of death pathways. Although AgNPs from various plant extracts have been studied, no existing publications report the use of I-AgNP for Saos-2 and MCF-7 cytotoxicity testing. Ozkan et al. have stated that methanol extract of *I. viscosa* showed an antiproliferative effect on human breast adenocarcinoma MCF-7 and brain cancer T98-G cell lines [45]. Virdis et al. showed that *Inula viscosa* extract exhibited strong antiproliferative and cytotoxic activities on the Raji Burkitt lymphoma cell line, arresting the cell cycle in the G2/M phase and causing an increase in cell apoptosis [46]. In addition to these mentioned studies, the antiproliferative effect of *Inula viscosa* has also been demonstrated in liver, lung, gastric and colon cancer cell lines [47–49]. While previous studies have reported the conjugation of *Inula viscosa* extract with silver nanoparticles [50], our work is the first to reveal their significant cytotoxic activity against MCF-7 and Saos-2 cells, highlighting their therapeutic potential. *Inula viscosa* contains sesquiterpene lactones

(e.g., tomentosin) and flavonoids that also elevate ROS levels and promote apoptotic signaling pathways [51]. A study by Merghoub et al. demonstrated that *Inula viscosa* extract induces oxidative stress-mediated apoptosis and telomere shortening in HeLa cells, mechanisms that may also operate in MCF-7 and Saos-2 cells. Literature also suggests that *Inula viscosa* alone can modulate apoptosis-related genes and proteins, including upregulation of Bax and downregulation of Bcl-2, favoring programmed cell death [17]. The presence of tomentosin and chlorogenic acid in *Inula viscosa* extract may further amplify DNA damage responses, leading to activation of p53 and downstream apoptosis effectors [52]. Synthesis of AgNPs using *Inula viscosa* extract allows improved colloidal stability and biological activity of these bioactive constituents, contributing synergistically to cytotoxicity by enhancing cellular uptake and triggering intracellular signaling cascades.

O-AgNPs demonstrated a dose- and time-dependent cytotoxicity in both MCF-7 and Saos-2 cell lines, although with relatively lower potency compared to *H. lupulus*- and *I. viscosa*-based AgNPs. Albogami et al. showed that *Olea europaea* leaf extract had a cytotoxic effect on HT-29 and PC3 cells [53]. Maalej et al. stated that *Olea europaea* fruit extract showed a cytotoxic effect in HepG2 and Caco-2 cells and arrested cells in the S phase [54]. Isleem et al. showed that the use of *Olea europaea* leaf extract in combination with metformin caused a stronger anticancer effect on the MCF-7 cells by modulating Bcl-2 family proteins, promoting pro-apoptotic Bax expression and downregulating anti-apoptotic Bcl-2. Oleuropein exhibits anti-inflammatory and anti-angiogenic properties by inhibiting NF-κB signaling and VEGF expression, respectively [55]. This is crucial for tumors such as osteosarcoma, where angiogenesis is a key driver of progression. In addition, there are studies in the literature about the effect of using O-AgNPs on cancer cell viability. It has been stated in studies that O-AgNPs have a stronger cytotoxic effect on breast, colon and cervical cancer [53, 56, 57]. While *Olea europaea* is rich in phenolic compounds like oleuropein and hydroxytyrosol, these compounds generally exert milder cytotoxicity compared to the more highly reactive sesquiterpene lactones in *Inula viscosa* or the prenylated flavonoids (e.g., xanthohumol) in *Humulus lupulus*. The latter are known to induce stronger pro-apoptotic, anti-proliferative, and ROS-generating effects, which may lead to more aggressive cancer cell killing [14, 15]. The reducing and capping agents derived from *Olea europaea* leaves may yield AgNPs with different surface properties (e.g., charge, hydrophilicity) than those capped with *I. viscosa* or *H. lupulus* extracts. This could result in lower cellular uptake or slower intracellular release of silver ions, thereby reducing bioavailability and cytotoxicity. Further studies focusing on the physicochemical properties of the AgNPs synthesized with different phytochemicals may help elucidate this postulation.

The results of this study demonstrated a dose- and time-dependent cytotoxic response of all three plant-mediated AgNPs against Saos-2 and MCF-7 cell lines. Notably, *Inula viscosa*-synthesized AgNPs exhibited the lowest IC_{50} values—0.25 mg/ml for Saos-2 and 0.37 mg/ml for MCF-7 after 48 h—indicating their superior cytotoxic potential among the tested formulations. In contrast, *Olea europaea*-derived AgNPs consistently required higher concentrations to elicit comparable effects, suggesting a milder cytotoxic profile. Importantly, at the lowest tested dilution (1:10), which corresponds to approximately 0.1–0.2 mg/ml depending on nanoparticle yield, cell viability remained comparatively high, particularly for MCF-7 cells.

These findings are consistent with previously reported studies indicating that green-synthesized AgNPs exhibit significant cytotoxicity at concentrations between 0.2 and 0.5 mg/ml, while lower concentrations ($\leq$ 0.1 mg/ml) tend to be less harmful to normal cells and may preserve therapeutic selectivity [53, 54]. For example, Das et al. reported an IC_{50} value of 0.147 mg/ml for hops-based AgNPs on MCF-7 cells, which closely parallels our findings for H-AgNPs [42]. This dose-dependent behavior underscores the importance of carefully defining therapeutic windows to optimize efficacy while minimizing potential off-target effects. Our data contribute to this emerging body of knowledge by providing comparative IC_{50} values and identifying relatively safe concentrations for further in vivo exploration.

This study demonstrates that plant-mediated silver nanoparticles, particularly those synthesized using *Inula viscosa*, exhibit significant dose- and time-dependent cytotoxic activity against Saos-2 and MCF-7 cancer cell lines. A comparative analysis of AgNPs derived from *Inula viscosa, Humulus lupulus*, and *Olea europaea* reveals that phytochemical composition, nanoparticle surface characteristics, and oxidative stress modulation collectively influence anticancer efficacy. Among the three, *Inula viscosa*-derived AgNPs showed the highest potency, while the distinct biological profiles of *Humulus lupulus* and *Olea europaea* formulations underscore the importance of plant selection in tailoring nanoparticles for specific therapeutic goals.

By applying a green synthesis protocol, this study systematically evaluates how different plant-derived phytochemicals impact nanoparticle properties and biological activity, rather than introducing a novel synthesis method. The findings validate the potential of green-synthesized AgNPs as promising, biocompatible alternatives to conventional chemotherapeutics, bridging traditional botanical knowledge with nanotechnology [58, 59]. This work advances academic understanding of plant-guided nanoparticle design while providing clinically relevant insights for targeted cancer treatment. Recent efforts to develop

cancer therapeutics with reduced systemic toxicity have led to growing interest in the use of phytochemicals derived from traditional medicine. Although these natural compounds exhibit promising biological activities against various malignancies, including breast cancer and osteosarcoma, their clinical translation remains limited due to poor pharmacokinetic properties, insufficient tumor selectivity, and low intracellular accumulation [60]. These challenges are particularly relevant for aggressive cancers such as MCF-7 breast cancer and Saos-2 osteosarcoma, which often exhibit resistance to conventional therapies. To overcome these obstacles, the integration of nanomaterials has emerged as a powerful strategy. Nanotechnology-based delivery systems can enhance the solubility, cellular uptake, and tumor-specific distribution of bioactive agents, thereby improving their therapeutic potential while minimizing adverse effects [61].

While this study provides valuable insights into the anticancer potential of plant-mediated silver nanoparticles (AgNPs), it has several important limitations. The findings are based solely on in vitro testing using Saos-2 and MCF-7 cancer cell lines, without considering the complex biological interactions that occur in vivo systems. Although UV–Vis, SEM, and XRD were used for nanoparticle characterization, advanced techniques like DLS, zeta potential measurement, and FTIR were not employed to thoroughly analyze particle size distribution, surface charge, and stability. Additionally, the mechanisms of cell death and selectivity profiles in healthy cells were not fully investigated. Future studies should incorporate in vivo models, pharmacokinetic analyses, and examinations of phytochemical synergistic effects to better understand the therapeutic potential of these plant-based nanoparticles.

Acknowledgements This study was carried out using the facilities of Ankara Yıldırım Beyazıt University, Central Research Laboratory Application and Research Center (MERLAB). A part of this study was presented in abstract form at the 6th International Conference on Advances in Natural and Applied Sciences (ICANAS) held in 2022.

Author Contributions T.O.S. conducted and performed experiments, analyzed the data, and drafted the manuscript. B. O. and M. G. performed experiments, analyzed data, and drafted the manuscript. T. A. collected the plant samples, contributed to the experiments, and manuscript drafting.

Funding Open access funding provided by the Scientific and Technological Research Council of Türkiye (TÜBİTAK).

Data Availability No datasets were generated or analysed during the current study.

Declarations

Conflict of Interest The authors declare no competing interests.

References

1. Sung H, Ferlay J, Siegel RL. Global cancer statistics: GLOBOCAN estimates of incidence and mortality worldwide for 36 cancers in 185 countries. CA Cancer J Clin. 2021. https://doi.org/10.3322/caac.21660.
2. Isakoff MS, Bielack SS, Meltzer P, Gorlick R. Osteosarcoma: current treatment and a collaborative pathway to success. J Clin Oncology. 2015. https://doi.org/10.1200/JCO.2014.59.4895.
3. Ping Y, Yajun M, Zheng Z. Multifunctional nanoparticles for the treatment and diagnosis of osteosarcoma. Biomater Adv. 2023. https://doi.org/10.1016/j.bioadv.2023.213466.
4. Uslu B, Yaman M, Sanci TÖ, Güngörmüş M, Köprü ÇZ, Güneş FE. Acetone extracts of Berberis vulgaris and Cornus mas L. induce apoptosis in MCF-7 breast cancer cells. Turk J Med Sci. 2023. https://doi.org/10.55730/1300-0144.5715.
5. Burguin A, Diorio C, Durocher F. Breast cancer treatments: updates and new challenges. J Personal Med. 2021. https://doi.org/10.3390/jpm11080808.
6. Sultana A, Zare M, Thomas V, Kumar TS, Ramakrishna S. Nano-based drug delivery systems: conventional drug delivery routes, recent developments and future prospects. Med Drug Discov. 2022. https://doi.org/10.1016/j.medidd.2022.100134.
7. Nejad FS, Alizade-Harakiyan M, Haghi M, Ebrahimi R, Zangeneh MM, Farajollahi A, Ahmadi A. Investigating the effectiveness of iron nanoparticles synthesized by green synthesis method in chemoradiotherapy of colon cancer. Heliyon. 2024. https://doi.org/10.1016/j.heliyon.2024.e28343.
8. Dias M, Zhang R, Lammers T, et al. Clinical translation and landscape of silver nanoparticles. Drug Deliv and Transl Res. 2025. https://doi.org/10.1007/s13346-024-01716-5.
9. Vahidi H, Kobarfard F, Alizadeh A, Saravanan M, Barabadi H. Green nanotechnology-based tellurium nanoparticles: Exploration of their antioxidant, antibacterial, antifungal and cytotoxic potentials against cancerous and normal cells compared to potassium tellurite. Inorg Chem Commun. 2021. https://doi.org/10.1016/j.inoche.2020.108385.
10. Duman H, Eker F, Akdaşçi E, Witkowska AM, Bechelany M, Karav S. Silver nanoparticles: a comprehensive review of synthesis methods and chemical and physical properties. Nanomaterials. 2024. https://doi.org/10.3390/nano14181527.
11. Gurunathan S, Kang MH, Jeyaraj M, Kim JH. Differential cytotoxicity of different sizes of graphene oxide nanoparticles in Leydig (TM3) and Sertoli (TM4) cells. Nanomaterials (Basel). 2019. https://doi.org/10.3390/nano9020139.
12. Moghaddam AB, Moniri M, Azizi S, et al. Eco-friendly formulated zinc oxide nanoparticles: induction of cell cycle arrest and apoptosis in the MCF-7 cancer cell line. Genes (Basel). 2017. https://doi.org/10.1016/j.inoche.2020.108385.

13. Dehnoee A, Javad KR, Zangeneh MM, Delnavazi MR, Zangeneh A. One-step synthesis of silver nanostructures using Heracleum persicum fruit extract, their cytotoxic activity, anti-cancer and anti-oxidant activities. Micro & Nano Letters. 2023. https://doi.org/10.1049/mna2.12153.
14. Iravani S, Korbekandi H, Mirmohammadi SV, Zolfaghari B. Synthesis of silver nanoparticles: chemical, physical and biological methods. Res Pharm Sci. 2014;9(6):385–406.
15. Ahmed S, Ahmad M, Swami BL, Ikram S. A review on plants extract mediated synthesis of silver nanoparticles for antimicrobial applications: a green expertise. J Adv Res. 2016. https://doi.org/10.1016/j.jare.2015.02.007.
16. Jiang CH, Sun TL, Xiang DX, Wei SS, Li WQ. Anticancer activity and mechanism of xanthohumol: a prenylated flavonoid from hops (Humulus lupulus L.). Front Pharmacol. 2018. https://doi.org/10.3389/fphar.2018.00530.
17. Merghoub N, El Btaouri H, Benbacer L, Gmouh S, Trentesaux C, Brassart B, Morjani H. Inula viscosa extracts induces telomere shortening and apoptosis in cancer cells and overcome drug resistance. Nutr Cancer. 2016. https://doi.org/10.1080/01635581.2016.1115105.
18. Rishmawi S, Haddad F, Dokmak G, Karaman RA. comprehensive review on the anti-cancer effects of oleuropein. Life (Basel). 2022. https://doi.org/10.3390/life12081140.
19. Güngörmüş M. Synthesis and characterization of silver nanoparticles using myrtus communis (myrtle) and grape seed extract. Gazi J Eng Sci. 2021;7(3):320–9.
20. Özalper B, Özdemir Sancı T, Özgüner HM. Antiproliferative effects of vitamin K2 in osteosarcoma cells: comparison of different cytotoxicity analyzes. Med J SDU. 2023. https://doi.org/10.17343/sdutfd.1099504.
21. Agnihotri S, Mukherji S, Mukherji S. Size-controlled silver nanoparticles synthesized over the range 5–100 nm using the same protocol and their antibacterial efficacy. ACS. 2014. https://doi.org/10.1039/C3RA44507K.
22. Majeed S, Saravanan M, Danish M, Zakariya NA, Ibrahim MNM, Rizvi EH, Mostafavi E. Bioengineering of green-synthesized TAT peptide-functionalized silver nanoparticles for apoptotic cell-death mediated therapy of breast adenocarcinoma. Talanta. 2023. https://doi.org/10.1016/j.talanta.2022.124026.
23. Prasannaraj G, Venkatachalam P. Hepatoprotective effect of engineered silver nanoparticles coated bioactive compounds against diethylnitrosamine induced hepatocarcinogenesis in experimental mice. J Photochem Photobiol B. 2017;167:309–20.
24. Prasannaraj G, Sahi SV, Ravikumar S, Venkatachalam P. Enhanced cytotoxicity of biomolecules loaded metallic silver nanoparticles against human liver (HepG2) and prostate (PC3) cancer cell lines. J Nanosci Nanotechnol. 2016. https://doi.org/10.1166/jnn.2016.12336.
25. Bai X, Tang J, Safaralizadeh R, Feizi MA, Delirezh N, Zangeneh A, Zangeneh MM. Green fabrication of bioactive copper nanoparticles using Acroptilon repens extract: an enhanced anti-lung cancer activity. Inorg Chem Commun. 2024;164: 112393.
26. Rudzińska A, Juchaniuk P, Oberda J, Wiśniewska J, Wojdan W, Szklener K, Mańdziuk S. Phytochemicals in cancer treatment and cancer prevention-review on epidemiological data and clinical trials. Nutrients. 2023. https://doi.org/10.3390/nu15081896.
27. George BP, Chandran R, Abrahamse H. Role of phytochemicals in cancer chemoprevention: insights. Antioxidants. 2021. https://doi.org/10.3390/antiox10091455.
28. Choudhari AS, Mandave PC, Deshpande M, Ranjekar P, Prakash O. Phytochemicals in cancer treatment: from preclinical studies to clinical practice. Front Pharmacol. 2020. https://doi.org/10.3389/fphar.2019.01614.
29. Xie J, Yang Z, Zhou C, Zhu J, Lee RJ, Teng L. Nanotechnology for the delivery of phytochemicals in cancer therapy. Biotechnol Adv. 2016. https://doi.org/10.1016/j.biotechadv.2016.04.002.
30. Kim B, Park JE, Im E, Cho Y, Lee J, Lee HJ, Kim SH. Recent advances in nanotechnology with nano-phytochemicals: molecular mechanisms and clinical implications in cancer progression. Int J Mol Sci. 2021. https://doi.org/10.3390/ijms22073571.
31. Tamia G, Amarakoon D, Wei CI, Lee SH. Evaluation of Humulus lupulus (hops) compound anti-proliferative properties with mechanisms in human colorectal cancer cells. Food Biosci. 2024. https://doi.org/10.1016/j.fbio.2023.103493.
32. Waterhouse GI, Bowmaker GA, Metson JB. The thermal decomposition of silver (I, III) oxide: a combined XRD, FT-IR and Raman spectroscopic study. Phys Chem Chem Phys. 2001. https://doi.org/10.1039/B103226G.
33. Besinis A, De Peralta T, Handy RD. The antibacterial effects of silver, titanium dioxide and silica dioxide nanoparticles compared to the dental disinfectant chlorhexidine on Streptococcus mutans using a suite of bioassays. Nanotoxicology. 2014. https://doi.org/10.3109/17435390.2012.742935.
34. Yang H, Ren YY, Wang T, Wang C. Preparation and antibacterial activities of Ag/Ag+/Ag3+ nanoparticle composites made by pomegranate (Punica granatum) rind extract. Results Phys. 2016. https://doi.org/10.1016/j.rinp.2016.05.012.
35. Ahmed S, Ahmad M, Swami BL, Ikram S. A review on plants extract mediated synthesis of silver nanoparticles for antimicrobial applications: a green expertise. J Adv Res. 2016. https://doi.org/10.1016/j.jare.2015.02.007.
36. Castro-Aceituno V, Ahn S, Simu SY, Singh P, Mathiyalagan R, Lee HA, Yang DC. Anticancer activity of silver nanoparticles from Panax ginseng fresh leaves in human cancer cells. Biomed Pharmacother. 2016. https://doi.org/10.1016/j.biopha.2016.09.016.
37. Arvizo RR, Bhattacharyya S, Kudgus RA, Giri K, Bhattacharya R, Mukherjee P. Intrinsic therapeutic applications of noble metal nanoparticles: past, present and future. Chem Soc Rev. 2012. https://doi.org/10.1039/C2CS15355F.
38. Monteiro R, Faria A, Azevedo I, Calhau C. Modulation of breast cancer cell survival by aromatase inhibiting hop (Humulus lupulus L.) flavonoids. J Steroid Biochem Mol Biol. 2007. https://doi.org/10.1016/j.jsbmb.2006.11.026.
39. Cömert Önder F, Ay M, Aydoğan Türkoğlu S, Tura Köçkar F, Celik A. Antiproliferative activity of Humulus lupulus extracts on human hepatoma (Hep3B), colon (HT-29) cancer cells and proteases, tyrosinase, β-lactamase enzyme inhibition studies. J Enzyme Inhib Med Chem. 2016. https://doi.org/10.3109/14756366.2015.1004060.
40. Caban M, Owczarek K, Chojnacka K, Podsędek A, Sosnowska D, Lewandowska U. Chemopreventive properties of spent hops (Humulus Lupulus L.) extract against angiogenesis, invasion and migration of colorectal cancer cells. J Physiol Pharmacol. 2022;73(3):431–42.
41. Ho YC, Liu CH, Chen CN, Duan KJ, Lin MT. Inhibitory effects of xanthohumol from hops (Humulus lupulus L.) on human hepatocellular carcinoma cell lines. Phytother Res: Int J Devoted Pharmacol Toxicol Eval Nat Prod Deriv. 2008. https://doi.org/10.1002/ptr.2481.
42. Das P, Dutta T, Manna S, Loganathan S, Basak P. Facile green synthesis of non-genotoxic, non-hemolytic organometallic silver nanoparticles using extract of crushed, wasted, and spent Humulus lupulus (hops): Characterization, anti-bacterial, and anti-cancer studies. Environ Res. 2022. https://doi.org/10.1016/j.envres.2021.111962.

43. Janicke RU, Sprengart ML, Wati MR, Porter AG. Caspase-3 is required for DNA fragmentation and morphological changes associated with apoptosis. J Biol Chem. 1998;273(16):9357–60.
44. Alowaiesh BF, Alhaithloul HAS, Saad AM, Hassanin AA. Green biogenic of silver nanoparticles using polyphenolic extract of olive leaf wastes with focus on their anticancer and antimicrobial activities. Plants. 2023. https://doi.org/10.3390/plants12061410.
45. Ozkan E, Karakas FP, Yildirim AB, Tas I, Eker I, Yavuz MZ, Turker AU. Promising medicinal plant Inula viscosa L.: Antiproliferative, antioxidant, antibacterial and phenolic profiles. Prog Nutr. 2019;21(3):652–61.
46. Virdis P, Migheli R, Galleri G, Fancello S, Cadoni MPL, Pintore G, Podda L. Antiproliferative and proapoptotic effects of Inula viscosa extract on Burkitt lymphoma cell line. Tumor Biology. 2020. https://doi.org/10.1177/1010428319901061.
47. Kheyar-Kraouche N, Boucheffa S, Bellik Y, Farida K, Brahmi-Chendouh N. Exploring the potential of Inula viscosa extracts for antioxidant, antiproliferative and apoptotic effects on human liver cancer cells and a molecular docking study. BioTechnologia (Pozn). 2023. https://doi.org/10.5114/bta.2023.127207.
48. Erdal B, Yılmaz B, Baylan B. Investigation of the antibacterial and anticarcinogenic effects of Inula viscosa methanol and hexane extracts. Turk Hijyen ve Deneysel Biyoloji Dergisi. 2022. https://doi.org/10.5505/TurkHijyen.2022.55798.
49. Okka EZ, Tongur Aytas TT, Yılmaz M, Topel Ö, Sahin R. Green synthesis and the formation kinetics of silver nanoparticles in aqueous Inula Viscosa extract. Optik. 2023. https://doi.org/10.1016/j.ijleo.2023.171487.
50. Bar-Shalom R, Bergman M, Grossman S, Azzam N, Sharvit L, Fares F. Inula viscosa extract inhibits growth of colorectal cancer cells in vitro and in vivo through induction of apoptosis. Front Oncol. 2019. https://doi.org/10.3389/fonc.2019.00227.
51. Merghoub N, Benbacer L, Terryn C, Attaleb M, Madoulet C, Benjouad A, Amzazi S. In vitro antiproliferative effect and induction of apoptosis by Retama monosperma L. extract in human cervical cancer cells. Cell Mol Biol. 2011. https://doi.org/10.5772/30025.
52. Rechek H, Haouat A, Hamaidia K, Pinto DC, Boudiar T, Válega MS, Silva AM. Inula viscosa (L.) aiton ethanolic extract inhibits the growth of human AGS and A549 cancer cell lines. Chem Biodiv. 2023. https://doi.org/10.1002/cbdv.202200890.
53. Albogami S, Hassan AM. Assessment of the efficacy of olive leaf (Olea europaea L.) extracts in the treatment of colorectal cancer and prostate cancer using in vitro cell models. Molecules. 2021. https://doi.org/10.3390/molecules26134069.
54. Maalej A, Bouallagui Z, Hadrich F, Isoda H, Sayadi S. Assessment of Olea europaea L. fruit extracts: Phytochemical characterization and anticancer pathway investigation. Biomed Pharmacother. 2017. https://doi.org/10.1016/j.biopha.2017.03.034.
55. Isleem RM, Alzaharna MM, Sharif FA. Synergistic anticancer effect of combining metformin with olive (Olea europaea L.) leaf crude extract on the human breast cancer cell line MCF-7. J Med Plants. 2020;8(2):30–7.
56. Alharbi NS, Felimban AI. Cytotoxicity of silver nanoparticles green-synthesized using Olea europaea fruit extract on MCF7 and T47D cancer cell lines. J King Saud Univ Sci. 2023. https://doi.org/10.1016/j.jksus.2023.102972.
57. Alhajri H, Alterary S, Alrfaei BM, Al-Qahtani WS. Therapeutic potential evaluation of green synthesized silver nanoparticles derived from olive (Olea europaea L.) leaf extracts against breast cancer cells. J Nanophoton. 2021. https://doi.org/10.1117/1.JNP.15.036003.
58. Han JW, Gurunathan S, Jeong JK. Oxidative stress mediated cytotoxicity of biologically synthesized silver nanoparticles in human lung epithelial adenocarcinoma cell line. Nanoscale Res Lett. 2014. https://doi.org/10.1186/1556-276X-9-459.
59. Nejad FS, Alizade-Harakiyan M, Haghi M, Ebrahimi R, Zangeneh MM, Farajollahi A, Ahmadi A. Investigation of the impact of copper nanoparticles coated with ocimum bassilicum at chemoradiotherapy of colon carcinoma. Biochem Biophys Rep. 2024;39:101780.
60. Li J, Mahdavi B, Baghayeri M, Rivandi B, Lotfi M, Zangeneh MM, Tayebee R. A new formulation of Ni/Zn bi-metallic nanocomposite and evaluation of its applications for pollution removal, photocatalytic, electrochemical sensing, and anti-breast cancer. Environ Res. 2023. https://doi.org/10.1016/j.envres.2023.116462.
61. Dehnoee A, Javad KR, Zangeneh MM, Delnavazi MR. One-step synthesis of silver nanostructures using Heracleum persicum fruit extract, their cytotoxic activity, anti-cancer and anti-oxidant activities. Micro Nano Lett. 2023. https://doi.org/10.1049/mna2.12153.